Article

Diketopiperazine Alkaloids and Bisabolene Sesquiterpenoids from *Aspergillus versicolor* AS-212, an Endozoic Fungus Associated with Deep-Sea Coral of Magellan Seamounts

Yu-Liang Dong [1,2,3], Xiao-Ming Li [1,2,4], Xiao-Shan Shi [1], Yi-Ran Wang [1,2,3], Bin-Gui Wang [1,2,3,4,*] and Ling-Hong Meng [1,2,3,4,*]

[1] CAS and Shandong Province Key Laboratory of Experimental Marine Biology, Institute of Oceanology, Chinese Academy of Sciences, Nanhai Road 7, Qingdao 266071, China; dongyuliang@qdio.ac.cn (Y.-L.D.); lixmqd@qdio.ac.cn (X.-M.L.); shixs@hbnu.edu.cn (X.-S.S.); wangyiran@qdio.ac.cn (Y.-R.W.)

[2] Laboratory of Marine Biology and Biotechnology, Qingdao National Laboratory for Marine Science and Technology, Wenhai Road 1, Qingdao 266237, China

[3] University of Chinese Academy of Sciences, Yuquan Road 19A, Beijing 100049, China

[4] Center for Ocean Mega-Science, Chinese Academy of Sciences, Nanhai Road 7, Qingdao 266071, China

[*] Correspondence: wangbg@ms.qdio.ac.cn (B.-G.W.); menglh@ms.qdio.ac.cn (L.-H.M.)

Abstract: Two new quinazolinone diketopiperazine alkaloids, including versicomide E (**2**) and cottoquinazoline H (**4**), together with ten known compounds (**1**, **3**, and **5–12**) were isolated and identified from *Aspergillus versicolor* AS-212, an endozoic fungus associated with the deep-sea coral *Hemicorallium* cf. *imperiale*, which was collected from the Magellan Seamounts. Their chemical structures were determined by an extensive interpretation of the spectroscopic and X-ray crystallographic data as well as specific rotation calculation, ECD calculation, and comparison of their ECD spectra. The absolute configurations of (−)-isoversicomide A (**1**) and cottoquinazoline A (**3**) were not assigned in the literature reports and were solved in the present work by single-crystal X-ray diffraction analysis. In the antibacterial assays, compound **3** exhibited antibacterial activity against aquatic pathogenic bacteria *Aeromonas hydrophilia* with an MIC value of 18.6 μM, while compounds **4** and **8** exhibited inhibitory effects against *Vibrio harveyi* and *V. parahaemolyticus* with MIC values ranging from 9.0 to 18.1 μM.

Keywords: diketopiperazine; *Aspergillus versicolor*; deep-sea coral; endophytic fungus; antimicrobial activity

1. Introduction

Marine-derived fungi living under extreme survival conditions are considered as abundant sources of structurally diverse and biologically active compounds [1,2]. In the deep-sea habitats, seamounts are regarded locations for a wide variety of current-topography interactions and biophysical coupling which have large biomass and higher biodiversity than their surrounding deep-sea floors [3,4]. Endozoic fungi surviving in deep-sea seamounts are a promising new source to mining bioactive secondary metabolites owing to their unique habitats. To date, only three papers investigating bioactive secondary metabolites of fungi derived from deep-sea seamounts have been published [5–7]. Therefore, a study on the chemical diversity of deep-sea seamount-derived endozoic fungi is warranted.

The species in the fungal genus *Aspergillus*, especially *A. versicolor*, is widely distributed in various habitats (marine, terrestrial, and symbiotic sources) and possesses the ability to produce diversified bioactive secondary metabolites such as diketopiperazine alkaloids [8,9], peptides [10], xanthones [9,11], and sesquiterpenes [12]. Most of these metabolites are described to exhibit a variety of bioactivities, including antifungal [9], antitumor [10,11], and neuroprotective activities [12].

In our continuous efforts to explore bioactive metabolites from deep-sea seamount-derived fungi [5–7], chemical investigation of the endozoic fungus *Aspergillus versicolor* AS-212 associated with the deep-sea coral, *Hemicorallium* cf. *imperiale*, which was collected from the Magellan Seamounts in the Western Pacific Ocean was carried out due to its unique HPLC profiles. As a result, two new quinazolinone diketopiperazine alkaloids, namely, versicomide E (**2**) and cottoquinazoline H (**4**), together with five known related analogs (**1**, **3**, **5–7**) as well as four known bisabolene derivatives (**8–11**) and a bisabolene dimer (**12**), have been isolated and identified. Herein, we report the isolation and structure elucidation as well as the antimicrobial activities of compounds **1–12** (Figure 1).
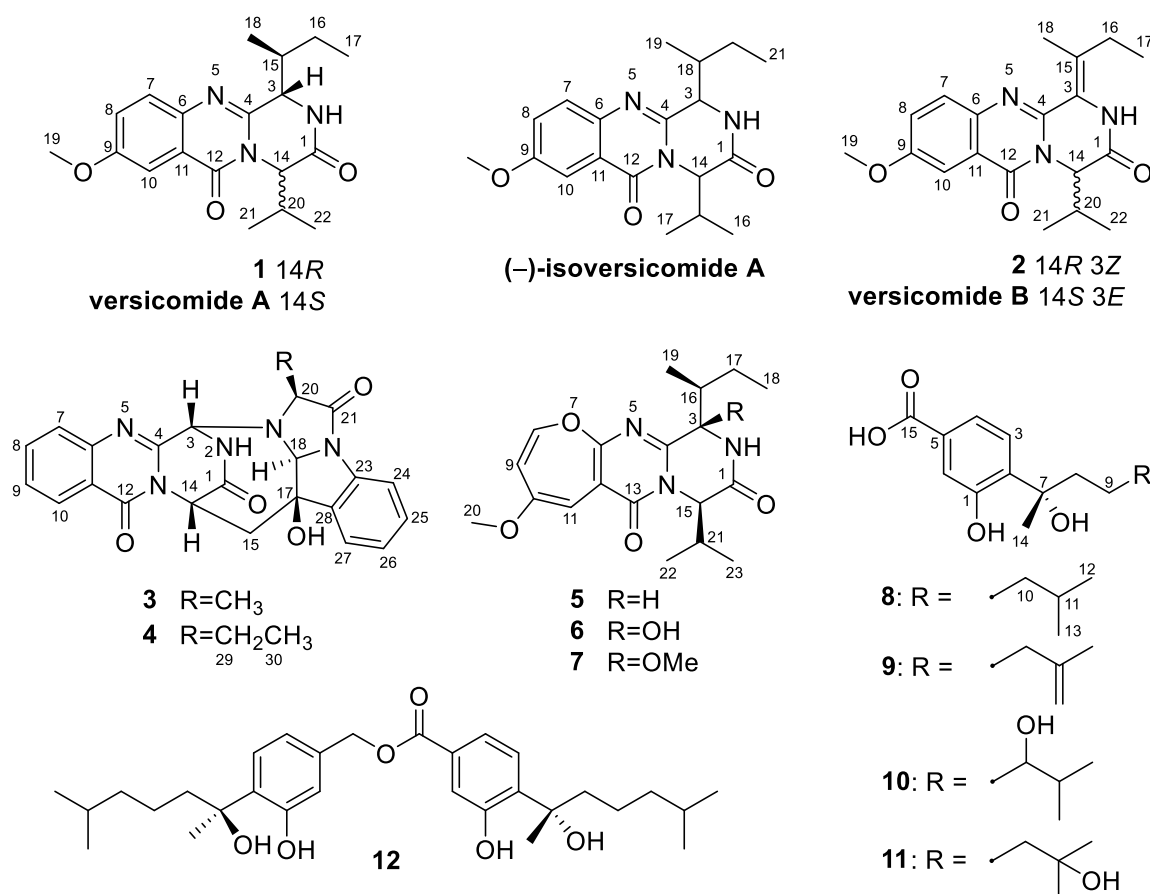
Figure 1. Structures of compounds **1–12**, versicomides A and B, and (−)-isoversicomide A.

2. Results and Discussion

2.1. Structure Elucidation of the Isolated Compounds

Compound **1** was isolated as colorless crystals, and the molecular formula was established as $C_{19}H_{25}N_3O_3$ by analysis of the HRESIMS data. The ^1H and ^{13}C NMR of **1** (DMSO-d_6, Table 1) extremely resembled those of versicomide A, a quinazoline-containing compound isolated from the crab-derived fungus *Aspergillus versicolor* XZ-4 which was collected from hydrothermal vent [8]. Further analysis of the 2D NMR spectra (Figure 2) indicated the same planar structure of **1** as that of versicomide A (Figure 1). However, a strong NOE cross-peak of H-3/H-20 was in favor of the structure with the 3*S**- and 14*R**-relative configuration rather than a 3*S** and 14*S** configuration (Figure 3). Single-crystal X-ray diffraction analysis with Cu Kα radiation further demonstrated its structure and absolute configurations (Figure 4). A Flack parameter of 0.0(2) enabled the definition of its absolute configuration as 3*S*, 14*R*, and 15*S*, indicating that **1** was the 14-epimer of versicomide A.

Table 1. ^{1}H (500 MHz) and ^{13}C (125 MHz) NMR Spectroscopic Data for Compounds **1** and **2**.

No.	Compound 1 [a]			Compound 2 [b]		
	δ_C, Type	δ_H (Mult, *J* in Hz)	HMBC (From H to C)	δ_C, Type	δ_H (Mult, *J* in Hz)	HMBC (From H to C)
1	168.0, C			167.1, C		
2		8.40, br s	1, 3, 4, 14		8.02, br s	4
3	58.1, CH	4.70, d (1.7)	4, 15, 16, 18	121.3, C		
4	149.3, C			144.3, C		
6	141.4, C			141.7, C		
7	129.5, CH	7.61, d (8.9)	9, 11	129.3, CH	7.62, d (8.9)	9, 11
8	124.9, CH	7.45, dd (8.9, 2.9)	6, 7, 10	125.1, CH	7.35, dd (8.9, 2.9)	6
9	158.5, C			159.0, C		
10	106.8, CH	7.52, d (2.9)	6, 8, 12	106.4, CH	7.65, d (2.9)	6, 8
11	120.9, C			120.8, C		
12	160.7, C			160.9, C		
14	60.9, CH	4.93, d (8.7)	1, 4, 12, 20	61.2, CH	5.33, dd (8.3, 1.5)	1, 4, 20
15	36.1, CH	2.62, m		135.0, C		
16	23.5, CH$_2$	1.34, m	15, 17	27.8, CH$_2$	2.29, m	3, 15
17	12.9, CH$_3$	0.86, overlap	15, 16	11.6, CH$_3$	1.15, t (7.6)	15, 16
18	15.5, CH$_3$	1.13, d (7.2)	3, 15, 16	19.5, CH$_3$	2.35, s	3, 15, 16
19	56.2, CH$_3$	3.88, s	9	56.0, CH$_3$	3.92, s	9
20	30.8, CH	2.26, m		32.2, CH	2.17, m	
21	20.2, CH$_3$	0.86, overlap	14, 20, 22	19.8, CH$_3$	1.01, d (6.8)	14, 20, 22
22	19.5, CH$_3$	1.04, d (6.6)	14, 20, 21	19.0, CH$_3$	1.09, d (6.8)	14, 20, 21

[a] Recorded in DMSO-d_6. [b] Recorded in CDCl$_3$.
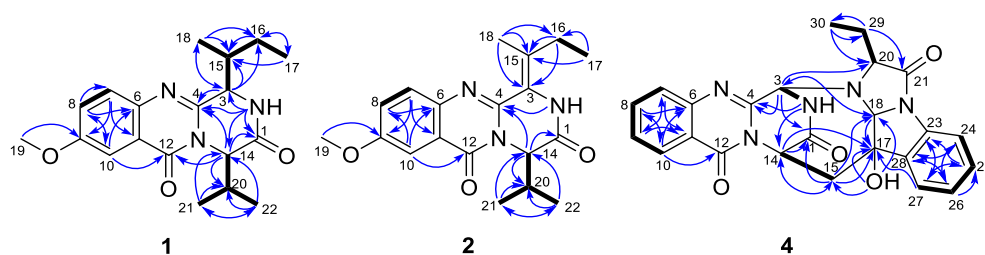
Figure 2. Key COSY (bold lines) and HMBC (blue arrows) correlations for compounds **1**, **2**, and **4**.
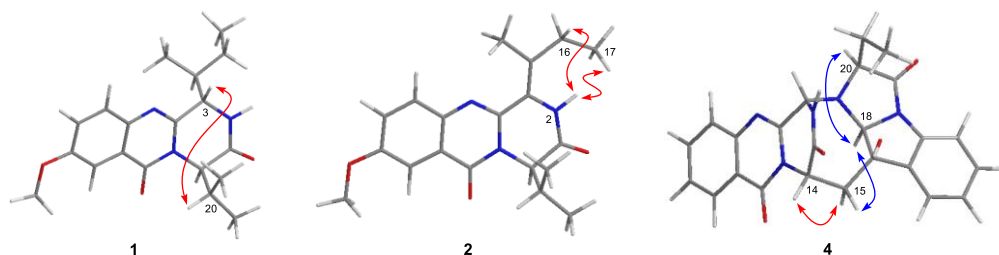
Figure 3. Key NOE correlations for compounds **1**, **2**, and **4** (red lines: *β*-orientation; blue lines: *α*-orientation).
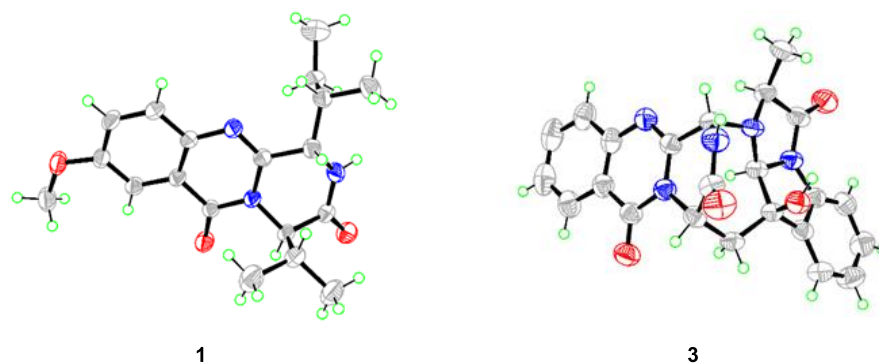
Figure 4. X-ray crystal structures of compounds **1** and **3**.

Compound **1** was initially treated as a new quinazoline alkaloid during the preparation of this manuscript, while Tasdemir and co-workers recently reported a new quinazoline-containing diketopiperazine (−)-isoversicomide A from the deep-sea sediment-derived fungus *Aspergillus versicolor* PS108-62 [13]. Notably, compound **1** shared the same planar structure and virtually similar optical rotation value ($[\alpha]_D^{25}$ −30 vs. $[\alpha]_D^{20}$ −25) as that of (−)-isoversicomide A, in which the stereogenic centers at C-3 and C-14 showed the same relative configurations with that of compound **1**. However, the configuration at C-18 on the short flexible aliphatic chain and the absolute configuration of (−)-isoversicomide A were not assigned due to the limited sample available [13]. Considering their similar rotation values and same relative configuration at C-3 and C-14, we assumed that compound **1** and (−)-isoversicomide A are the same compound. As the reported evidence to determine the absolute configuration of versicomide A does not seem entirely solid and in view of the highly similar NMR data of those isomers with multi-chiral centers, it is necessary to clarify the absolute configuration of **1**. The results from the X-ray diffraction analysis of compound **1** unambiguously determined its absolute configuration as 3*S*, 14*R*, and 15*S*. This is likely the first time the configuration of isoleucine in a quinazoline-containing diketopiperazine skeleton with a Val-Ile cyclic dipeptide moiety was unambiguously defined by X-ray crystallography analysis.

Versicomide E (**2**) was obtained as a colorless amorphous solid with the molecular formula $C_{19}H_{23}N_3O_3$ based on the HRESIMS data. Its NMR data (CDCl$_3$, Table 1) were similar to those of **1**, which indicated that **2** possessed the same quinazoline backbone as **1**. The obvious difference was the absence of signals for two methines at δ_C 58.1/δ_H 4.70 (CH-3) and δ_C 36.1/δ_H 2.62 (CH-15) in the NMR spectra of **1**, whereas additional resonances corresponding to a tetra-substituted double bond at δ_C 121.3 (C-3) and δ_C 135.0 (C-15) were found in that of **2** (CDCl$_3$, Table 1), which were further confirmed by COSY and HMBC correlations (Figure 2). The geometry of the double bond between C-3 and C-15 was determined as Z-configuration by key NOE correlations from NH-2 (δ_H 8.02) to H-16 (δ_H 2.29) and H$_3$-17 (δ_H 1.15) (Figure 3). Compound **2** has the same planar structure as that of versicomide B (Figure 1), which was also isolated from hydrothermal vent crab-derived fungus *Aspergillus versicolor* XZ-4 by Wu and co-workers in 2017 [8], with the exception of the geometry of the double bond at C3(15) (Z in **2** vs. E in versicomide B) and the absolute configuration of C-14 (R in **2** vs. S in versicomide B) as well. To clarify the stereochemistry of compound **2**, calculations of specific rotation (SR) were carried out for 14*R*-**2** and 14*S*-**2**, and the calculated SR value for 14*R*-**2** (+59.8) at CAM-B3LYP/TZVP level was compatible with the experimental SR value $[\alpha]_D^{25}$ +112.0 (*c* 0.08, MeOH), contrary to that of versicomide B ($[\alpha]_D^{20}$ −23.4) [8], which allowed the assignment of absolute configuration of C-14 in **2** as 14*R* (Table S2). To further verify the absolute configuration of C-14 in **2**, the time-dependent density functional (TDDFT)-ECD calculation was performed on 14*R*-**2** and 14*S*-**2** at the CAM-B3LYP/TZVP level in Gaussian 09. The experimental curve matched that of the calculated ECD spectrum for 14*R*-**2** and also assigned the absolute configuration of C-14 in **2** as 14*R* (Figure S27).

Compound **3** was obtained as colorless prisms and was identified as cottoquinazoline A by comparing its NMR data (measured in DMSO-d_6, Table S3) with those previously reported in the literature [10]. Cottoquinazoline A is a 16-nor analog of the known fumiquinazoline D and was first isolated from a marine-derived fungal strain of *A. versicolor* (MST-MF495) by Capon and co-workers in 2009, with a partial stereostructure assigned [10]. Considering the complexity of the structure of **3** and the presence of many stereoisomers, it is important to clarify the assignment of the absolute configurations of **3** [10,14]. Fortunately, a suitable crystal of **3** was picked out from DMSO–MeOH (1:1) and subjected to X-ray crystallographic analysis to assign its absolute configurations of the stereogenic centers in **3** as 3*S*, 14*S*, 16*R*, 17*S*, and 19*S* (Figure 4).

Cottoquinazoline H (**4**) was obtained as a colorless amorphous solid. Its molecular formula was established as $C_{24}H_{21}N_5O_4$ by HRESIMS, with one CH$_2$ unit more than that of **3**. Discreet comparisons of the NMR data (DMSO-d_6, Table 2) and UV absorptions with

3 suggested that they shared the same core scaffold. However, the methyl substitution at C-20 in **3** was replaced by an ethyl group in **4**, as evidenced by the appearance of an additional methylene group resonating at δ_C 21.0 and δ_H 1.90/1.99 (CH$_2$-29) in the NMR spectra of **4** (DMSO-d_6, Table 2). Additionally, the chemical shift of C-20 was deshielded downfield from δ_C 63.2 in **3** to δ_C 68.1 in **4**. The COSY and HMBC correlations verified the above deduction (Figure 2). The relative configuration of **4** was also deduced from the analysis of NOESY experiments. The NOE cross-peaks from H-20 and H-15α to H-18 revealed the cofacial orientation of these groups (Figure 3). Given that the stereochemistry of co-isolated compound **3** was determined by X-ray diffraction analysis as well as their similar NMR chemical shifts and virtually identical experimental ECD curves (Figure 5), the absolute configurations of all chiral carbons in **4** were established as 3*S*, 14*S*, 17*R*, 18*S*, and 20*S*.

Table 2. ^{1}H (500 MHz) and ^{13}C (125 MHz) NMR data for compound **4** (in DMSO-d_6).

No.	δ_C, Type	δ_H (Mult, *J* in Hz)	HMBC (From H to C)
		Compound 4	
1	167.8, C		
2		9.10, d, (5.1)	4, 14
3	65.4, CH	5.22, d, (5.1)	1, 4, 18, 20
4	147.4, C		
6	146.7, C		
7	127.2, CH	7.74, dd, (8.4,1.0)	9, 11
8	134.4, CH	7.84, ddd, (8.4, 7.1, 1.5)	6, 10
9	127.1, CH	7.55, ddd, (8.1, 7.1, 1.0)	7, 11
10	126,1, CH	8.13, dd, (8.0, 1.5)	6, 8, 12
11	120.7, C		
12	159.3, C		
14	53.8, CH	5.27, dd, (5.3, 2.4)	1, 15, 17
15	36.3, CH$_2$	3.08, dd, (14.9, 5.3)	17, 18
		2.42, dd, (14.9, 2.4)	1, 14
17	73.9, C		
18	79.6, CH	4.87, d (1.8)	3, 17
20	68.1, CH	4.06, m	
21	164.6, C		
23	135.9, C		
24	113.6, CH	7.29, overlap	26, 28
25	129.3, CH	7.29, overlap	23, 27
26	124.3, CH	7.09, ddd (7.6, 4.2, 3.4)	24, 25, 28
27	124.4, CH	7.42, d, (7.6)	17, 25
28	139.6, C	-	
29	21.0, CH$_2$	1.90, m	21, 30
		1.99, m	
30	8.9, CH$_3$	1.06, t, (7.4)	20, 29
17-OH		5.35, s	15, 17, 18

In addition to compounds **1–4**, three related quinazolinone diketopiperazine alkaloids, namely, versicoloids A and B (**5** and **6**) [9], and chrysopiperazine A (**7**) [15], as well as five known bisabolene derivatives (**8–12**) including sydonic acid (**8**) [16], (*S*)-(+)-11-dehydrosydonic acid (**9**) [17], (−)-10-hydroxysydonic acid (**10**) [18], hydroxysydonic acid (**11**) [16], and peniciaculin B (**12**) [18] were also identified and isolated from the fungus *A. versicolor* AS-212, which were determined by the comparison of their NMR data and those previously described in the literature. Structurally, (−)-isoversicomide A (**1**) might be a plausible biosynthetic precursor that undergoes the transformation of the benzene ring to the oxepine ring to generate versicoloid A (**5**) [19], which provides the basis for the biosynthetic origins of versicoloid A.
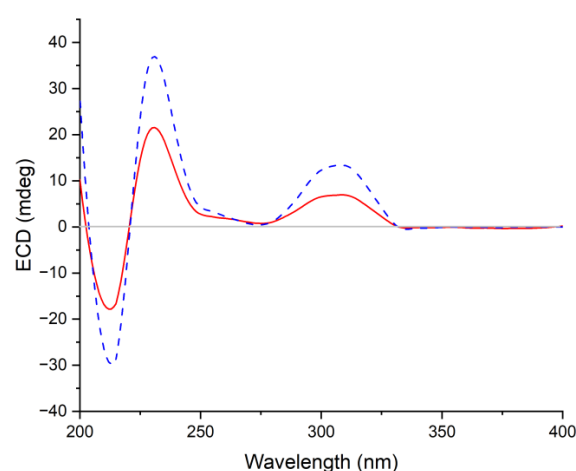
Figure 5. Comparison of the experimental ECD spectra of compounds **3** (in red) and **4** (in blue) in CH$_3$OH.

2.2. Antimicrobial Assays

The antimicrobial activity evaluation of all the isolated compounds was performed against human pathogenic bacterium (*Escherichia coli*), marine-derived aquatic pathogenetic bacteria (*Aeromonas hydrophila*, *Edwardsiella ictarda*, *Micrococcus luteus*, *Pseudomonas aeruginosa*, *Vibrio harveyi*, *V. parahemolyticus*, *V. vulnificus*), and plant-pathogenic fungi (*Colletotrichum gloeosporioides*, *Curvularia spicifera*, *Epicoccum sorghinum*, *Fusarium oxysporum*, *F. proliferatum*, and *Penicillium digitatum*) (Table 3). In the antimicrobial screening, compounds **4** and **8** exhibited potent inhibitory activity against the aquatic pathogenic bacterium *V. parahaemolyticus* with MIC values of 9.0 and 15.0 μM, while compounds **8** and **9** showed inhibitory activity against the aquatic pathogenic bacterium *V. harveyi* with the MIC values of 15.0 and 15.2 μM. In addition, compounds **3** and **4** displayed a broad spectrum of antimicrobial activity against most of the tested strains, with the MIC values ranging from 9.0 to 74.6 μM. The bisabolene derivatives (**8–12**) mainly exhibited activities against *M. luteus*, *V. harveyi*, and *V. parahemolyticus*, with MIC values ranging from 15.0 to 121.2 μM. However, neither the quinazoline-containing diketopiperazine derivatives (**1** and **2**) nor the oxepine-containing diketopiperazine analogs (**5–7**) showed any activity against all the tested pathogenic bacteria. These data suggested that the 16-*nor*-methyl fumiquinazoline alkaloids generally showed higher antimicrobial activity than that of quinazolinone alkaloids (**3** and **4** vs. **1** and **2**) and the oxepine congeners (**5–7**). A comparison of the antimicrobial results of **3** and **4** revealed that different substituent groups at C-20 could influence the inhibitory potency against the pathogenic bacteria. Concerning bisabolene derivatives, the antimicrobial results revealed that compound **12**, a dimeric bisabolene analog, showed weaker antimicrobial activities than that of the monomeric bisabolenes (**8–11**) against *M. luteus* and *V. harveyi*. In addition, hydroxylation at C-10 or C-11 likely decreased the activity against *V. harveyi*, *V. parahaemolyticus*, and *C. gloeosporioides* (**8** vs. **10** and **11**).

Table 3. The antimicrobial activities of compounds **1–12** (MIC, μM) [a].

Strains	1	2	3	4	5	6	7	8	9	10	11	12	Positive Control
A. hydrophila	-	-	18.6	-	-	-	-	-	-	-	-	-	6.2 [b]
E. coli	-	-	-	72.2	-	-	-	-	-	-	-	-	6.2 [b]
M. luteus	-	-	74.6	36.1	-	-	-	-	-	-	-	-	3.1 [b]
V.harveyi	-	-	37.3	18.1	-	-	-	15.0	15.2	28.4	-	-	3.1 [b]
V. parahaemolyticus	-	-	37.3	9.0	-	-	-	15.0	121.2	113.5	113.5	64.0	3.1 [b]
V. vulnificus	-	-	74.6	72.2	-	-	-	-	-	-	-	-	3.1 [b]
C. spicifera	93.3	187.7	74.6	72.2	-	170.1	-	-	-	-	-	-	1.1 [c]
C. gloeosporioides	186.6	-	74.6	72.2	89.1	170.1	164.5	120.3	121.2	-	-	-	2.2 [c]

[a] (-) = MIC > 200 μM; Positive control: [b] Chloromycetin; [c] amphotericin B.

The above results showed that compounds **4**, **8**, and **9** were found to be efficient in suppressing the growth of aquatic pathogenic bacteria *V. parahaemolyticus* and *V. harveyi*. To a great degree, the endozoic fungus *A. versicolor* AS-212 which is associated with the deep-sea coral *Hemicorallium* cf. *imperiale* may provide a chemical defense to help its host to fight off the aquatic pathogenic bacteria by producing an array of antimicrobial secondary metabolites.

3. Experimental Section

3.1. General Experimental Procedures

The general experimental procedures, apparatus, and solvents/reagents used in this work were the same as those described in our previous reports [5–7].

3.2. Fungal Material

The endophytic fungus *Aspergillus versicolor* AS-212 associated with deep-sea coral, *Hemicorallium* cf. *imperial*, was collected from the Magellan Seamounts (depth 1420 m) in May 2018. By comparing its ITS region sequence with that of *A. versicolor* (accession no. MT582751.1) in the GenBank database, the sequence data of strain AS-212 were identical (100%) to those of *A. versicolor* and subsequently uploaded in GenBank with accession no. OP009765.1. The fungus AS-212 has been conserved at the Key Laboratory of Experimental Marine Biology, Institute of Oceanology, Chinese Academy of Sciences (IOCAS).

3.3. Fermentation, Extraction, and Isolation

The fungal strain AS-212 was cultivated on potato dextrose agar (PDA) plates at 28 °C for 7 days to generate spores. The fresh mycelia were transferred into 1 L Erlenmeyer flasks, each containing 300 mL potato-dextrose broth (PDB) medium, which was reported in our previous publication [5], and fermented under static conditions for 30 days at room temperature. After 30 days of incubation, a total of 33 L cultures were filtered and collected to separate the broth and mycelia. The broth was adequately extracted three times with EtOAc, while the mycelia were mechanically crushed and then extracted three times with 80% volume aqueous acetone. Acetone was removed in vacuo to afford an aqueous solution, which was successively extracted with EtOAc. Based on their virtually similar TLC and HPLC profiles (Figure S26), both EtOAc extracts from broth and mycelia were combined and evaporated under a vacuum to render the EtOAc extract (61 g).

The EtOAc extract was subjected to vacuum liquid chromatography (VLC) eluted with petroleum ether (PE)–EtOAc gradient (20:1 to 1:1, *v/v*) and then CH_2Cl_2–MeOH (20:1 to 1:1, *v/v*) to afford nine fractions (Frs. 1–9). Fr. 4 (2.3 g) was fractionated by reverse-phase column chromatography (CC) with a MeOH–H_2O gradient (from 10:90 to 100:0) to afford nine subfractions (Frs.4.1–4.9). Fr. 4.2 was directly purified by semi-preparative HPLC (Elite ODS-BP, 5μm; 10 × 250 mm; 80% MeOH–H_2O, 2.5 mL/min) to yield compound **6** (3.0 mg, t_R = 17 min). Fr. 4.4 (16 mg) was further purified by prep. TLC (plate: 20 × 20 cm, developing solvents: PE–EtOAc, 2:1) and by Sephadex LH-20 (MeOH) column to afford **7** (3.1 mg). Fr. 4.5 was purified by CC over Sephadex LH-20 chromatography (MeOH) and then by semi-preparative HPLC (85% MeOH–H_2O, 2.5 mL/min) to give compound **1** (6.6 mg, t_R = 14 min). Fr. 4.6 (75 mg) was fractionated by CC on Sephadex LH-20 column (MeOH) to yield five subfractions Frs.4.6.1–4.6.5. Fr. 4.6.5 (20 mg) was further purified by prep. TLC (developing solvents: DCM–MeOH, 20:1) and by Sephadex LH-20 (MeOH) to afford compound **9** (7.7 mg). Fr. 4.7 (36 mg) was directly purified by prep. TLC (developing solvents: CH_2Cl_2–EtOAc, 3:1) and by Sephadex LH-20 (MeOH) to afford compound **8** (4.0 mg). Fr. 4.8 (67 mg) was purified by CC on silica gel eluting with CH_2Cl_2–MeOH gradient (from 200:1 to 50:1) to obtain compound **12** (4.3 mg). Fr. 5 (3.4 g) was separated by reversed-phase CC using step-gradient elution with MeOH–H_2O (from 10:90 to 100:0) to yield seven subfractions (Frs. 5.1–5.7). Fr. 5.2 (241 mg) was fractionated by CC on silica gel eluting with CH_2Cl_2–MeOH gradient (from 150:1 to 20:1) and then purified on Sephadex LH-20 (MeOH) to afford compounds **10** (11.3 mg) and **11** (4.3 mg). Fr. 5.4 (126 mg) was fractionated by CC on Sephadex LH-20 (MeOH) and further purified by

semi-preparative HPLC (70% MeOH–H$_2$O, 2.5 mL/min) to afford compound **5** (6.3 mg, t_R = 22 min). Fr. 5.6 was chromatographed via a Sephadex LH-20 column (MeOH) and then by semi-preparative HPLC (78% MeOH-H$_2$O, 2.5 mL/min) to afford compound **2** (6.7 mg, t_R = 20 min). Fr. 7 (5.8 g) was fractionated by reverse-phase CC with a MeOH–H$_2$O gradient (from 10:90 to 100:0) to yield five subfractions (Frs. 7.1–7.5). Fr. 7.5 (328 mg) was applied to silica gel CC eluted with CH$_2$Cl$_2$/MeOH to give nine subfractions (Frs. 7.5.1–7.5.9). Fr.7.5.7 (36 mg) was purified by semi-preparative HPLC (45% MeCN–H$_2$O, 2.5 mL/min) to provide compounds **3** (4.3 mg, t_R = 9 min) and **4** (3.2 mg, t_R = 12 min).

(−)-Isoversicomide A (**1**): colorless crystals; mp 197−199 °C; $[\alpha]_D^{25}$ −30 (*c* 0.10, MeOH); UV (MeOH) λ_{max} (log ε) 227 (3.47), 277 (3.00), 326 (2.58) nm; ECD (0.52 mM, MeOH) λ_{max} ($\Delta\varepsilon$) 210 (−4.87), 233 (−15.03), 277 (+1.88), 328 (−1.02) nm; for ^{1}H and ^{13}C NMR data, see Table 1; HRESIMS *m/z* 344.1960 [M + H]$^+$ (calcd for C$_{19}$H$_{26}$N$_3$O$_3$, 344.1969).

Versicomide E (**2**): colorless amorphous solid; $[\alpha]_D^{25}$ +112 (*c* 0.08, MeOH); UV (MeOH) λ_{max} (log ε) 221 (3.26), 309 (2.88) nm; ECD (0.59 mM, MeOH) λ_{max} ($\Delta\varepsilon$) 207 (+6.69), 233 (−3.87), 255 (+6.18), 300 (+1.41), 343 (−1.15) nm; for ^{1}H and ^{13}C NMR data, see Table 1; HRESIMS *m/z* 340.1663 [M − H]$^-$ (calcd for C$_{19}$H$_{22}$N$_3$O$_3$, 340.1667).

Cottoquinazoline A (**3**): colorless prisms (MeOH-DMSO 1:1); mp 215−217 °C; $[\alpha]_D^{25}$ +160 (*c* 0.10, MeOH); UV (MeOH) λ_{max} (log ε) 205 (3.39), 227 (3.17), 256 (2.81), 268 (2.74), 280 (2.68), 305 (2.26), 315 (2.14) nm; ECD (0.58 mM, MeOH) λ_{max} ($\Delta\varepsilon$) 211 (−13.16), 230 (+12.22), 308 (+3.60) nm; for ^{1}H and ^{13}C NMR data, see Table S2.

Cottoquinazoline H (**4**): colorless amorphous solid; $[\alpha]_D^{25}$ +150 (*c* 0.10, MeOH); UV (MeOH) λ_{max} (log ε) 205 (3.60), 227 (3.43), 257 (3.11), 270 (3.03), 279 (2.96), 304 (2.52), 317 (2.40) nm; ECD (0.56 mM, MeOH) λ_{max} ($\Delta\varepsilon$) 212 (−22.91), 231 (+21.65), 308 (+7.16) nm; for ^{1}H and ^{13}C NMR data, see Table 2; HRESIMS *m/z* 444.1663 [M + H]$^+$ (calcd for C$_{24}$H$_{22}$N$_5$O$_4$, 444.1666).

3.4. X-ray Crystallographic Analysis of Compounds **1** and **3**

Suitable crystals were picked out to obtain crystallographic data using a Bruker Smart-1000 or Bruker D8 VENTURE CCD diffractometer with Cu Kα radiation (λ = 1.54178 Å). Absorption correction was applied using the program SADABS [20]. The structures were solved by direct methods with the SHELXTL software package [21,22]. All non-hydrogen atoms were refined anisotropically. The absolute structures were determined by refinement of the Flack parameter [23]. The structures were optimized by full-matrix least-squares techniques. Crystallographic data have been deposited with the Cambridge Crystallographic Data Centre with deposition numbers CCDCs 2192654 and 2192653 for **1** and **3**, respectively. Crystal data and structure refinements for **1** and **3** are listed in Table S1.

Crystal data for compound 1: C$_{19}$H$_{25}$N$_3$O$_3$, F.W. = 343.2, space group P2(1)2(1)2(1), unit cell dimensions a = 13.2384(3) Å, b = 19.9347(4) Å, c = 6.8103(2) Å, V = 1797.26(8) Å^3, α = β = γ = 90°, Z = 4, d$_{calcd}$ = 1.269 g/cm^3, crystal dimensions 0.350 × 0.330 × 0.300 mm, μ = 0.702 mm^{-1}, F(000) = 736. The 4007 measurements yielded 2826 independent reflections after equivalent data were averaged. The final refinement gave R$_1$ = 0.0379 and wR$_2$ = 0.0989 [I > 2σ(I)]. Flack parameter = 0.0(2).

Crystal data for compound 3: 2(C$_{23}$H$_{18}$N$_5$O$_4$)·C$_2$OS$_2$, F.W. = 960.99, orthorhombic space group C222$_1$, unit cell dimensions a = 9.4022(11) Å, b = 25.878(4) Å, c = 19.112(2) Å, V = 4650.2(11) Å^3, α = β = γ = 90°, Z = 4, d$_{calcd}$ = 1.373 g/cm^3, crystal dimensions 0.200 × 0.180 × 0.150 mm, μ = 1.612 mm^{-1}, F(000) = 1992. The 21,138 measurements yielded 4267 independent reflections after equivalent data were averaged. The final refinement gave R$_1$ = 0.0951 and wR$_2$ = 0.2851 [I > 2σ(I)]. Flack parameter = 0.145(12).

3.5. Antimicrobial Assay

A two-fold serial dilution method using 96-well microtiter plates was applied to evaluating the antimicrobial activities against a panel of aquatic pathogenic bacteria (*Aeromonas hydrophilia* QDIO-1, *Edwardsiella ictarda* QDIO-9, *Micrococcus luteus* QDIO-3, *Pseudomonas*

aeruginosa QDIO-4, *Vibrio harveyi* QDIO-7, *V. parahaemolyticus* QDIO-8, and *V. vulnificus* QDIO-10), one human pathogenic bacterium (*Escherichia coli* EMBLC-1), and six plant-pathogenic fungi (*Penicillium digitatum* QDAU-3, *Colletotrichum gloeosporioides* QA-29, *Fusarium oxysporum* QDAU-8, *Curvularia spicifera* QA-26, *Epicoccum sorghinum* QA-20, and *F. proliferatum* QA-28) [24]. The aquatic pathogenic strains and human pathogenic bacterium were provided by IOCAS, while the plant-pathogenic fungi were provided by IOCAS and Qingdao Agricultural University. To assay the antimicrobial activities, DMSO was added to dissolve all isolated compounds and positive control (chloramphenicol and amphotericin B) to prepare a stock solution with a specific concentration.

3.6. Specific Rotation and ECD Calculations

General computational procedures were consistent with our previous reports [5,25].

4. Conclusions

In conclusion, two new quinazolinone derivatives, versicomide E (**2**) and cottoquinazoline H (**4**), along with ten known compounds (**1**, **3**, and **5**–**12**), were isolated and identified from the deep-sea coral-derived *Aspergillus versicolor* AS-212. This marks the first time that the absolute configurations of all the stereogenic centers in (−)-isoversicomide A (**1**) and cottoquinazoline A (**3**), which were not assigned in the previous literature, were accurately solved in the present work by X-ray crystallographic analysis. Compound **3** exhibited activity against aquatic pathogenic bacteria *A. hydrophilia* with an MIC value of 18.6 μM, while compounds **4** and **8**–**10** exhibited inhibitory effects against *V. harveyi* with MIC values ranging from 15.0 to 28.4 μM. In addition, compounds **4** and **8** exhibited potent inhibitory effects against *V. parahaemolyticus* with MIC values of 9.0 and 15.0 μM, which might have the potential to be developed as leading compounds in discovering aquatic antibiotics.

Supplementary Materials: The following supporting information can be downloaded at: https://www.mdpi.com/article/10.3390/md21050293/s1, Figures S1–S27: The analyzed data of MS, 1D and 2D NMR spectra of compounds **1**–**4**, crystal packing of compounds **1** and **3**, HPLC analysis of mycelia extract, broth extract, and compounds **1**–**12** of *Aspergillus versicolor* AS-212, and experimental and calculated ECD spectra of compound **2** at the CAM-B3LYP/TZVP level. Table S1: Crystal data and structure refinement for compounds **1** and **3**. Table S2: Calculated specific rotation values at 589.44 nm for the enantiomers 14*R*-**2** and 14*S*-**2** at the CAM-B3LYP/TZVP level. Table S3: ^{1}H and ^{13}C NMR spectroscopic data for compound **3**.

Author Contributions: Y.-L.D. performed the experiments for the extraction, isolation, structure elucidation, and bioactivity evaluation and prepared the manuscript; X.-M.L. performed the 1D and 2D NMR experiments; X.-S.S. and Y.-R.W. contributed to the isolation, identification, and small-scale screening of the fungus AS-212. L.-H.M. contributed to NMR analysis and structure elucidation; B.-G.W. supervised the research work and revised the manuscript. All authors have read and agreed to the published version of the manuscript.

Data Availability Statement: Not applicable.

Conflicts of Interest: The authors declare no conflict of interest.

References

1. Newman, D.J.; Cragg, G.M. Natural products as sources of new drugs over the nearly four decades from 01/1981 to 09/2019. *J. Nat. Prod.* **2020**, *83*, 770–803. [CrossRef]
2. Wang, Y.N.; Meng, L.H.; Wang, B.G. Progress in research on bioactive secondary metabolites from deep-sea derived microorganisms. *Mar. Drugs* **2020**, *18*, 614. [CrossRef]

3. Xu, K.D. Exploring seamount ecosystems and biodiversity in the tropical Western Pacific Ocean. *J. Oceanol. Limnol.* **2021**, *39*, 1585–1590. [CrossRef]

4. Clark, M.R.; Rowden, A.A.; Schlacher, T.; Williams, A.; Consalvey, M.; Stocks, K.I.; Rogers, A.D.; O'Hara, T.D.; White, M.; Shank, T.M. The ecology of seamounts: Structure, function, and human impacts. *Annu. Rev. Mar. Sci.* **2010**, *2*, 253–278. [CrossRef] [PubMed]

5. Meng, L.H.; Li, X.M.; Zhang, F.Z.; Wang, Y.N.; Wang, B.G. Talascortenes A–G, highly oxygenated diterpenoid acids from the sea-anemone-derived endozoic fungus *Talaromyces scorteus* AS-242. *J. Nat. Prod.* **2020**, *83*, 2528–2536. [CrossRef] [PubMed]

6. Hu, X.Y.; Li, X.M.; Wang, B.G.; Meng, L.H. Tanzawaic acid derivatives: Fungal polyketides from the deep-sea coral-derived endozoic *Penicillium steckii* AS-324. *J. Nat. Prod.* **2022**, *85*, 1398–1406. [CrossRef]

7. Hu, X.Y.; Li, X.M.; Wang, B.G.; Meng, L.H. Uncommon polyketides from *Penicillium steckii* AS-324, a marine endozoic fungus isolated from deep-sea coral in the Magellan seamount. *Int. J. Mol. Sci.* **2022**, *23*, 6332. [CrossRef]

8. Pan, C.Q.; Shi, Y.T.; Chen, X.G.; Chen, C.A.; Tao, X.Y.; Wu, B. New compounds from a hydrothermal vent crab-associated fungus *Aspergillus versicolor* XZ-4. *Org. Biomol. Chem.* **2017**, *15*, 1155–1163. [CrossRef]

9. Wang, J.F.; He, W.J.; Huang, X.L.; Tian, X.P.; Liao, S.R.; Yang, B.; Wang, F.Z.; Zhou, X.J.; Liu, Y.H. Antifungal new oxepine-containing alkaloids and xanthones from the deep-sea-derived fungus *Aspergillus versicolor* SCSIO 05879. *J. Agric. Food Chem.* **2016**, *64*, 2910–2916. [CrossRef]

10. Fremlin, L.J.; Piggott, A.M.; Lacey, E.; Capon, R.J. Cottoquinazoline A and cotteslosins A and B, metabolites from an Australian marine-derived strain of *Aspergillus versicolor*. *J. Nat. Prod.* **2009**, *72*, 666–670. [CrossRef]

11. Yu, G.H.; Wu, G.W.; Sun, Z.C.; Zhang, X.M.; Che, Q.; Gu, Q.Q.; Zhu, T.J.; Li, D.H.; Zhang, G.J. Cytotoxic tetrahydroxanthone dimers from the mangrove-associated fungus *Aspergillus versicolor* HDN1009. *Mar. Drugs* **2018**, *16*, 335. [CrossRef] [PubMed]

12. Weng, H.Z.; Zhu, J.Y.; Yuan, F.Y.; Tang, Z.Y.; Tian, X.Q.; Chen, Y.; Fan, C.Q.; Tang, G.H.; Yin, S. Homo/Hetero-dimers of aromatic bisabolane sesquiterpenoids with neuroprotective activity from the fungus *Aspergillus versicolor* A18 from South China Sea. *Mar. Drugs* **2022**, *20*, 322. [CrossRef] [PubMed]

13. Magot, F.; Van Soen, G.; Buedenbender, L.; Li, F.J.; Soltwedel, T.; Grauso, L.; Mangoni, A.; Blümel, M.; Tasdemir, D. Bioactivity and metabolome mining of deep-sea sediment-derived microorganisms reveal new hybrid PKS-NRPS macrolactone from *Aspergillus versicolor* PS108-62. *Mar. Drugs* **2023**, *21*, 95. [CrossRef]

14. Lin, S.; Yu, H.M.; Yang, B.Y.; Li, F.L.; Chen, X.; Li, H.Q.; Zhang, S.T.; Wang, J.P.; Hu, Y.C.; Hu, Z.X.; et al. Reisolation and configurational reinvestigation of cottoquinazolines E–G from an arthropod-derived strain of the fungus *Neosartorya fischeri*. *J. Nat. Prod.* **2020**, *83*, 169–173. [CrossRef]

15. Xu, W.F.; Mao, N.; Xue, X.J.; Qi, Y.X.; Wei, M.Y.; Wang, C.Y.; Shao, C.L. Structures and absolute configurations of diketopiperazine alkaloids chrysopiperazines A–C from the gorgonian-derived *Penicillium chrysogenum* fungus. *Mar. Drugs* **2019**, *17*, 250. [CrossRef]

16. Hamasaki, T.; Nagayama, K.; Hatsuda, Y. Two new metabolites, sydonic acid and hydroxysydonic acid, from *Aspergillus sydowi*. *Agric. Biol. Chem.* **1978**, *42*, 37–40. [CrossRef]

17. Lu, Z.Y.; Zhu, H.J.; Fu, P.; Wang, Y.; Zhang, Z.H.; Lin, H.P.; Liu, P.P.; Zhuang, Y.B.; Hong, K.; Zhu, W.M. Cytotoxic polyphenols from the marine-derived fungus *Penicillium expansum*. *J. Nat. Prod.* **2010**, *73*, 911–914. [CrossRef]

18. Li, X.D.; Li, X.M.; Xu, G.M.; Zhang, P.; Wang, B.G. Antimicrobial phenolic bisabolanes and related derivatives from *Penicillium aculeatum* SD-321, a deep sea sediment-derived fungus. *J. Nat. Prod.* **2015**, *78*, 844–849. [CrossRef]

19. Zheng, L.J.; Wang, H.W.; Fan, A.L.; Li, S.M. Oxepinamide F biosynthesis involves enzymatic D-aminoacyl epimerization, 3*H*-oxepin formation, and hydroxylation induced double bond migration. *Nat. Commun.* **2020**, *11*, 4914. [CrossRef]

20. Sheldrick, G.M. *SADABS, Software for Empirical Absorption Correction*; University of Göttingen: Göttingen, Germany, 1996.

21. Sheldrick, G.M. *SHELXTL, Structure Determination Software Programs*; Bruker Analytical X-ray System Inc.: Madison, WI, USA, 1997.

22. Sheldrick, G.M. *SHELXL-97 and SHELXS-97, Program for X-ray Crystal Structure Solution and Refinement*; University of Göttingen: Göttingen, Germany, 1997.

23. Parsons, S.; Flack, H.D.; Wagner, T. Use of intensity quotients and differences in absolute structure refinement. *Acta Crystallogr. Sect. B Struct. Sci. Cryst. Eng. Mater.* **2013**, *B69*, 249–259. [CrossRef]

24. Pierce, C.G.; Uppuluri, P.; Tristan, A.R.; Wormley, F.L.; Mowat, E.; Ramage, G.; Lopez-Ribot, J.L. A simple and reproducible 96-well plate-based method for the formation of fungal biofilms and its application to antifungal susceptibility testing. *Nat. Protoc.* **2008**, *3*, 1494–1500. [CrossRef] [PubMed]

25. Yan, L.H.; Li, P.H.; Li, X.M.; Yang, S.Q.; Liu, K.C.; Wang, B.G.; Li, X. Chevalinulins A and B, proangiogenic alkaloids with a spiro [bicyclo [2.2. 2] octane-diketopiperazine] skeleton from deep-sea cold-seep-derived fungus *Aspergillus chevalieri* CS-122. *Org. Lett.* **2022**, *24*, 2684–2688. [CrossRef] [PubMed]